Band-gap modification of defective carbon nanotubes under a transverse electric field

Li-Gan Tien,[1] Chuen-Horng Tsai,[1] Feng-Yin Li,[2,*] and Ming-Hsien Lee[3]

[1]*Department of Engineering and System Science, National Tsing Hua University, HsinChu, Taiwan 300, Republic of China*

[2]*Department of Chemistry, National Chung Hsing University, Taichung, 420, Taiwan, Republic of China*

[3]*Department of Physics, Tamkang University, Tamsui, Taipei 25137, Taiwan, Republic of China*

(Received 6 May 2005; revised manuscript received 18 July 2005; published 15 December 2005)

Ab initio calculations show that the band-gap modulation of semiconducting carbon nanotubes with mono-vacancy defect can be easily achieved by applying a transverse electric field. We found that the band structures of the defective carbon nanotubes vary quite differently from that of the perfect nanotube, and strongly depend on the applied direction of the transverse electric field. A mechanism is proposed to explain the variation of the band gap, and potential applications of these phenomena are discussed.

DOI: 10.1103/PhysRevB.72.245417 PACS number(s): 73.22.−f, 73.63.Fg, 71.15.Mb

I. INTRODUCTION

Single-walled carbon nanotubes (SWNTs) have emerged as attractive materials for molecular electronic applications[1,2] since their discovery in 1991.[3] Depending sensitively on its diameter and chirality, a SWNT can demonstrate either metallic or semiconducting conduction, suggesting a variety of electronic applications.[4,5] Among them, the SWNT field-effect transistor (SWNTFET) is a promising candidate for future electronic devices since the current in SWNTs can be switched on or off by an external electric field. Several groups have demonstrated such functional FETs successfully[5–7] and the electronic structures of the SWNTs under external electric field have been also calculated theoretically.[8–11] Recently, the polarizabilities of SWNTs under an external transverse electric field was calculated by both Hartree-Fock (HF) and density functional theory (DFT) to discuss the possibility of using SWNTs as shielding for nanoelectrical components.[12] Most experimental and theoretical investigations have focused on defect-free SWNTs with perfect honeycomb carbon arrangement, even though several experimental results have revealed that structural defects are commonly present in nanotubes.[13–15] Theoretical calculations have shown that structural defects in SWNTs, such as topological defects, vacancies, and chemical modifications, can substantially modify their electronic properties.[16–23] Recently, with improvement of experimental techniques, direct observation of the atomic-scale defects in graphene layers has enabled us to investigate the physical and chemical properties of defective carbon nanostructures in detail.[15,24–28] An electrochemical process developed by Fan *et al.*[28] to control these defects makes the design of reliable carbon nanotube electronic circuits possible. However, experimental characterizations for the role of defects in SWNTFETs are only beginning to emerge,[29] and many theoretical predictions remain to be tested. In order to demonstrate the influence of the atomic defects on the application of SWNTFETs, we report the band structure of a semiconducting SWNT with a mono-vacancy defect under a transverse electric field based on first-principle total energy and electric structure calculations.

II. MODEL AND CALCULATION METHOD

In order to facilitate the computation, a single-wall (10,0) nanotube with a mono-vacancy defect was modeled by 8 layers of carbon rings (80 carbon atoms) with one carbon atom missing to represent the vacancy defect. Systematic analyses were performed to investigate the variation of the electronic properties of defected SWNTs, such as band-gap modification and charge redistribution under a transverse electric field in various directions. The simulated model was placed within a tetragonal supercell with the lattice constants of a, b, and c. The lattice constant a and b were equal to 20 Å to avoid the interaction between two adjacent nanotubes. The lattice constant c along the tube axis was taken to be equal to the one-dimensional lattice parameter of the nanotube. The nanotube was taken along the z axis and the circular cross section was lying in the (x,y) plane. The vacancy site of the defective nanotube was chosen to sit on the $+x$ axis. Density functional theory calculations were performed with the CASTEP code.[30] Except where explicitly mentioned, the typical calculation setting is the following. The calculations were done with geometry optimization in generalized gradient approximation (GGA).[31,32] The structure of the defected nanotube was fully optimized until the force on each atom during the relaxation was less than 0.005 eV Å^{-1}. The nuclei and core electrons were represented by ultrasoft pseudopotentials.[33]

The summation over 1D Brillouin zone with wave vectors varying only along the tube axis was carried out with k-point sampling using a Monkhorst-Pack grid.[34] The fast-Fourier-transform (FFT) grid is set to be $90\times90\times40$ and a kinetic energy cutoff of 240 eV and 12 k points were used along the z axis to ensure convergence in the calculation. To study the effect of the transverse electric field on the electronic structure of the nanotube, the potential generated by the external electric field along the x (or y) direction (perpendicular to the tube axis) is modeled as a sawtoothlike potential, i.e.,

$$V_{ext}(r) = |e|Ex \quad (0 < x \leqslant L), \tag{1}$$

where E is the magnitude of the external electric field and L is the size of the supercell, chosen large enough so that the tube is located at the center of the supercell to avoid discon-

 ©2005 The American Physical Society

TABLE I. The band-gap variation of a zigzag (10,0) SWNT under a transverse electric field applied +x-axis direction.

Field	0	0.125	0.25	0.375	0.5	0.55	0.6	0.65	0.7	0.75
A[a]	0.67	0.67	0.65	0.63	0.56	0.55	0.54	0.41	0.21	0.00
B	0.19	0.25	0.31	0.37	0.36	0.34	0.31	0.28	0.21	0.00
C	0.30	0.35	0.40	0.45	0.48	0.49	0.50	0.42	0.38	0.09

[a]The first row is the applied field strength +x direction with unit as V/Å. The rows A, B, and C are the band gaps under a given field strength for the 80-atom perfect, 79-atom defective, and 119-atom defective nanotubes. The unit of the bandgap is electron volts.

tinuity at the supercell boundary. This external real-space potential is conveniently added into the total Kohn-Sham potential at the stage of constructing exchange-correlation potential on real-space grids. The validity of using such a simple implementation of finite electric field for a nonperiodic setup was already demonstrated by early density functional calculations,[35] which showed that the charge screening of the external electric field can be well described simply by changing the slope of the external potential.

III. RESULT AND DISCUSSION

In order to examine the effect of the mono-vacancy defect on the semiconductor-metal transition of the nanotube, two more models besides the original defective nanotube were also tested: a perfect (10,0) nanotube with 80 carbon atoms and a similar defective (10,0) nanotube but with 119 carbon atoms. After geometry optimization and band structure calculations with the various strengths of the transverse electric field in the +x direction, the band gaps of these three nanotubes were obtained, and are listed in Table I. For the band-gap variation of the perfect nanotube, our results share a similar trend with those obtained by Chen *et al.*[36] However, some differences exist between our results and theirs. For example, in low field strength up to 0.375 V/Å, our band gaps are consistently smaller than theirs. Somehow, in our results, the decay of the band gap along with the increase of the field strength is slower than that found in the results of Chen *et al.*,[36] and therefore the semiconductor-metal transition in our calculation requires higher field strength (0.75 V/Å) than that found in their results (0.6 V/Å). As for the response of the vacancy-defective nanotubes toward the transverse electric field, there are two interesting phenomena observed. First, the semiconductor-metal transition does exist regardless of the vacancy-defect concentration; however, the band-gap variations are quite different between the perfect and vacancy-defective nanotubes, indicating a strong effect caused by the vacancy defect. Second, the band-gap variations for the two defective models share a similar trend, even though the exact values of the band gaps under various strengths of the external transverse field are different, showing the dependence on the vacancy-defect concentration. We will elaborate upon these findings later. To facilitate the calculation, we decided to use the 79-atom defective nanotube as our study model from now on.

The band-gap variation of the defective nanotube under a transverse electric field with different applied directions was summarized in Fig. 1. The band gap of the defective nanotube is 0.19 eV at the Γ point of the Brillouin zone, smaller than that of the corresponding perfect nanotube found in Table I and also smaller than those found in the previous calculations.[36,37] As in the perfect nanotube under external transverse electric field, there exists a semiconductor-metal

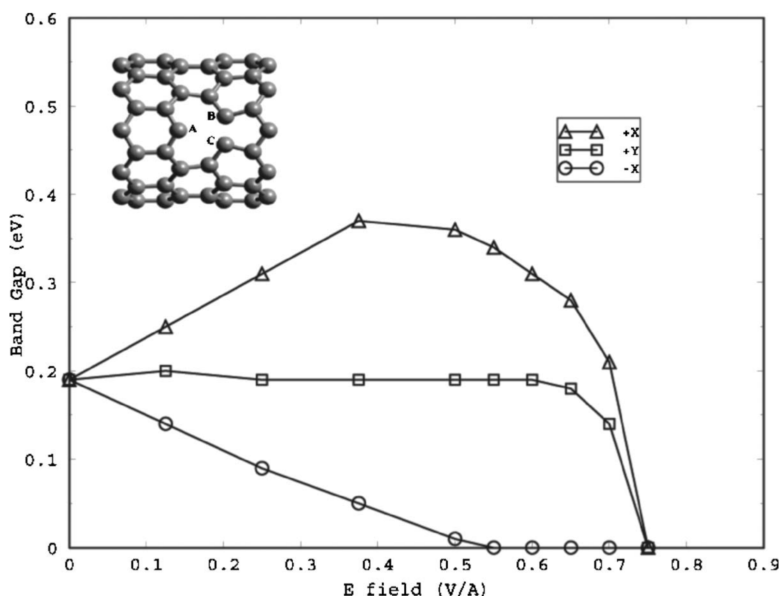

FIG. 1. The variation of the band gap for the defective (10,0) nanotube with 79 carbon atoms under a transverse electric field applied in three different directions, +x-axis, −x-axis, and y-axis, where the triangles represent the electric field in +x axis, squares are in +y axis, and circles are in −x axis. The inset plot is its optimized structure where A, B, and C are the nearest neighbors to the vacancy site.

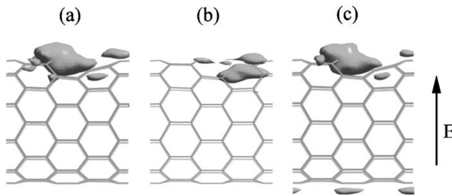

FIG. 2. The orbital density plots of the defective nanotube. (a) The unperturbed density of the CBM state, which is composed mostly of P_z orbitals around the vacancy site. (b) The unperturbed density of the VBM state, which is composed mostly of P_x and P_y orbitals around the vacancy site. (c) The density of the CBM state under a $+x$-axis electric field with 0.5 V/Å. The arrow indicates the direction of the external electric field.

transition when the transverse electric field strength reaches a certain value for all the simulated models. However, the variations of the band gaps along with the strength of the transverse electric field are quite different among them. Unlike the band gap of the perfect nanotube which decreases monotonously with the increase of the field strength before reaching the semiconductor-metal transition,[36] that of the defective nanotube, along with the increase of the field strength, can either increase first and later decrease, or first hold almost constant and then decrease, or decrease monotonously before reaching the semiconductor-metal transition. It is interesting to note that the critical field strengths to reach semiconductor-metal transition are also different among the different applied directions. For the $+x$- and $+y$-axis fields, the transition strengths are the same, 0.75 V/Å, while that in the $-x$-axis field, which is a negative electric field compared to the $+x$-axis field, is around 0.50 V/Å instead. Obviously, the above phenomena indicate that the electric properties of the defective nanotube strongly depend on the applied direction of the transverse electric field. The underlying mechanisms for band-gap shrinkage could be very complicated. In order to elucidate the physics governing the band-gap shrinkages of the defective nanotube in various directions of the external field, we analyzed their band structures, partial/projected density of state (PDOS), and the charge densities of the valence band maximum (VBM) and conduction band minimum (CBM) states. The VBM state is mostly contributed by P_x and P_y orbitals for all the simulated models, similar to that found in the corresponding perfect nanotube [see Fig. 2(b) for detail]. As shown in Fig. 2(a) and Fig. 3, we found that, without the external electric field, the CBM state of the defective nanotube is mostly composed of the P_z orbitals, acting like a doped state, contributed predominantly by the three carbon atoms around the defect site, and the state immediately lying above those P_z orbitals is the lowest conduction π^* state, the CBM state for the perfect nanotube. From now on, we denote this state as the P_z-orbital state. This explains the reason why the band gap of the defective nanotube is smaller than that of the corresponding perfect one. From the band structures of the defective nanotube unperturbed and under an external electric field as shown in Fig. 4, we found the P_z-orbital state shows an upward shift with a $+x$-axis field, but remains almost unchanged with the increase of the field strength from the $+y$ axis. However, a downward shift is found with a $-x$-axis field. It indicates that

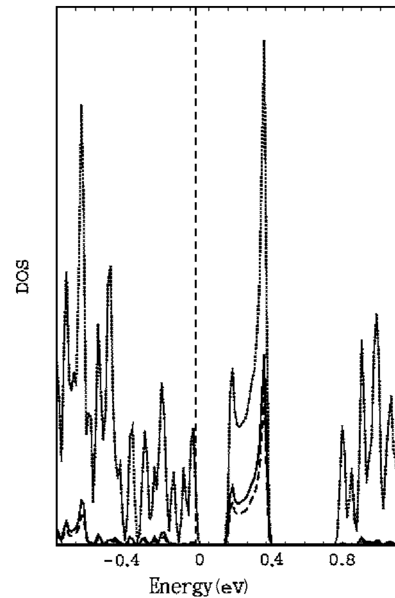

FIG. 3. The total density of state (TDOS) and partial density of state (PDOS) for the defective nanotube without electric field, where the dot line represents the TDOS; the black line is the P_z PDOS of all the carbon atoms; the dashed line presents the P_z PDOS of the three nearest carbon atoms around the vacancy site; and the vertical line represents the Fermi level.

the P_z-orbital state is strongly influenced by the direction of the charge polarization caused by the external electric field. Similar to those found in the previous studies for the perfect nanotubes,[36] the conduction π^* states also show a downward shift as the field strength increases no matter of the applied direction, as shown in Figs. 4(b) and 4(c).

Through the shift of those states mentioned above caused by the external electric field, we construct the underlying mechanisms of the band-gap shrinkage for the defective nanotube. The P_z-orbital state and the lowest conduction π^* state move close to each other and eventually cross over, when the direction of the external electric field is applied from the $+x$ or $+y$ axis. However, the energy difference between the P_z-orbital state and the lowest conducting π^* state shrinks more rapidly in the $+x$-axis field than the $+y$-axis as the field strength increases. When the lowest conduction π^* state and the P_z-orbital state move close to each other, subband mixing between them becomes more pronounced as the $+x$-axis field strength increases beyond 0.4 V/Å [see Fig. 2(c)], and the band gap starts to shrink. As for the $+y$-axis external electric field, the subband mixing between the above states is not pronounced as that found in the $+x$-axis field because the field polarization effect in the $+y$-axis field does not influence the P_z-orbital state significantly. As the field strength increases in both the $+x$-axis and the $+y$-axis fields, the lowest conduction π^* state eventually replaces the P_z-orbital state as the CBM state, and the behavior of the band-gap shrinkage becomes similar to that found in the corresponding perfect nanotube after this crossover. However, in the $-x$-axis field, the situation is different since the downward shift of the P_z-orbital state makes the semiconductor-metal transition happen before the subband mixing with the

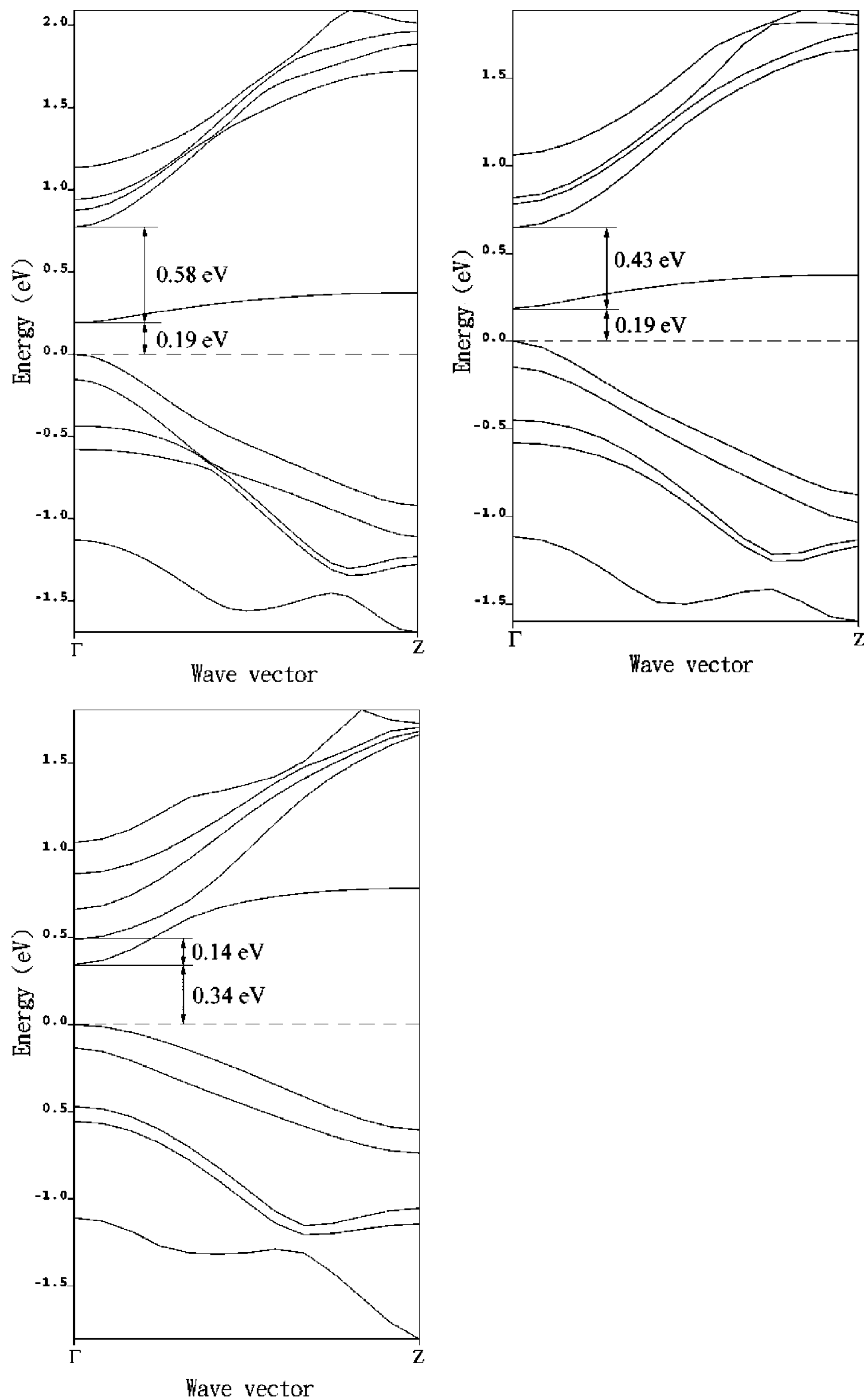

FIG. 4. The band structures of the defective nanotube under a transverse electric field, where the dashed lines represent the Fermi level. (a) The unperturbed band structure. (b) The band structure of the defective nanotube under a +*x*-axis electric field with 0.5 V/Å. (c) The band structure of the defective nanotube under a *y*-axis electric field with 0.5 V/Å. The energy difference between the lowest and second lowest conducting bands shrinks more rapidly in the +*x*-axis than in the *y*-axis.

lowest conduction π^* state can take place. It is the reason why its critical field strength of the semiconductor-metal transition is shorter than that found in the other two models. From our results, a general trend of the band-gap shrinkage for a semiconducting nanotube with a mono-vacancy defect under a transverse electric field can be obtained. When a

nanotube with the above characteristics is rotated in an external electric field with the setting similar to the simulated model, its band gap will vary and the maximum and minimum values of the band gap will be found when the direction of the applied field is corresponding to the $+x$ axis and $-x$ axis in our study, respectively, provided the field strength is not too high.

With the above knowledge, one can modulate the band gap of a semiconducting nanotube with vacancy defects within a certain range by changing the field strength and direction of the transverse electric field for specific applications. Another important application is that one can determine the existence of vacancy defects in a semiconducting nanotube by simply rotating the nanotube in a transverse electric field. Besides, if the band gap varies according to the direction of the external electric field, the direction with the maximum of the band gap will be the direction of the nanotube where the possible vacancy sites reside.

IV. CONCLUSION

We have demonstrated successfully that a zigzag (10,0) SWNT with a mono-vacancy defect responds quite differently toward a transverse electric field with different applied directions. The defect site of the defective nanotube provides a CBM with lower energy than that found in the corresponding perfect nanotube. The response of the P_z-orbital state, contributed mostly by the nearest carbon atoms to the vacancy site, toward the different applied directions of an external electric field is the main reason for the difference of the band-gap variations for the nanotubes with vacancy defects. Our results indicate that the band gap can be modulated by rotating a semiconducting nanotube with a mono-vacancy defect under a transverse electric field with various field strengths. With large field strength, the band-gap variation becomes similar to that found in the corresponding perfect nanotubes. If one rotates a mono-vacancy nanotube under a transverse electric field, the minimum and maximum of the band gap can indicate possible locations of the vacancy sites. This also provides some flexibility to select a suitable band gap for some specific applications since the band gap can increase or decrease depending on the direction and strength of the transverse electric field.

ACKNOWLEDGMENTS

The authors would like to acknowledge the National Center for High-Performance Computing, Taiwan for providing computational resources. Financial support from the National Science Council of Taiwan is gratefully acknowledged. F.Y.L. acknowledges the support of NSC 94-2113-M-005-002 and M.H.L. thanks the support of NSC 94-2112-M-032-015.

---

*Email address: feng64@nchu.edu.tw

[1] C. Dekker, Phys. Today **52**, 22 (1999).
[2] T. W. Odom, J.-L. Huang, P. Kim, and C. M. Lieber, J. Phys. Chem. B **104**, 2794 (2000).
[3] S. Ijima, Nature (London) **354**, 56 (1991).
[4] M. A. Reed and J. M. Tour, Sci. Am. **282**, 86 (2000).
[5] S. T. Tans, R. M. Verschueren, and C. Dekker, Nature (London) **393**, 49 (1998).
[6] R. Martel, T. Schmidt, H. R. Shea, T. Hertel, and P. Avouris, Appl. Phys. Lett. **73**, 2447 (1998).
[7] C. Zhou, J. Kong, and H. Dai, Appl. Phys. Lett. **76**, 1597 (1999).
[8] L. Lou, P. Nordlander, and R. E. Smalley, Phys. Rev. B **52**, 1429 (1995).
[9] C. Kim, B. Kim, S. M. Lee, C. Jo, and Y. H. Lee, Appl. Phys. Lett. **79**, 1187 (2001).
[10] A. Rochefort, M. D. Ventra, and P. Avouris, Appl. Phys. Lett. **78**, 2521 (2001).
[11] Y. Li, S. V. Rotkin, and U. Ravaioli, Nano Lett. **3**, 183 (2003).
[12] E. N. Brothers, K. N. Kudin, G. E. Scuseria, and C. W. Bauschlicher, Phys. Rev. B **72**, 033402 (2005).
[13] T. W. Ebbesen and T. Takada, Carbon **33**, 973 (1995).
[14] D. B. Mawhinney, V. Naumenko, A. Kuznetsova, J. T. Yates, J. Liu, and R. E. Smalley, Chem. Phys. Lett. **324**, 213 (2000).
[15] A. Hashimoto, K. Suenaga, A. Gloter, K. Urita, and S. Ijima, Nature (London) **430**, 870 (2004).
[16] J.-C. Charlier, T. W. Ebbesen, and P. Lambin, Phys. Rev. B **53**, 11108 (1996).
[17] V. H. Crespi, M. L. Cohen, and A. Rubio, Phys. Rev. Lett. **79**, 2093 (1997).
[18] L. Chico, M. P. LopezSancho, and M. C. Munoz, Phys. Rev. Lett. **81**, 1278 (1998).
[19] T. Kostyrko, M. Bartkowiak, and G. D. Mahan, Phys. Rev. B **60**, 10735 (1999).
[20] A. Hansson, M. Paulsson, and S. Stafstrom, Phys. Rev. B **62**, 7639 (2000).
[21] M. Bockrath, W. Liang, D. Bozovic, J. H. Hafner, C. M. Lieber, M. Tinkham, and H. Park, Science **291**, 283 (2001).
[22] C. P. Ewels, M. I. Heggie, and P. R. Briddon, Chem. Phys. Lett. **351**, 178 (2002).
[23] A. J. Lu and B. C. Pan, Phys. Rev. Lett. **92**, 105504 (2004).
[24] K. Urita, K. Suenaga, T. Sugai, H. Shinohara, and S. Iijima, Phys. Rev. Lett. **94**, 155502 (2005).
[25] A. J. Lu and B. C. Pan, Phys. Rev. B **71**, 165416 (2005).
[26] Y. C. Ma, P. O. Lehtinen, A. S. Foster, and R. M. Nieminen, New J. Phys. **6**, 68 (2004).
[27] C. Gomez-Navarro, P. J. De Pablo, J. Gomez-Herrero, B. Biel, F. J. Garcia-Vidal, A. Rubio, and F. Flores, Nat. Mater. **4**, 534 (2005).
[28] Y. Fan, N. Emmott, and P. G. Collins, Technical Proceedings of the 2005 NSTI Nanotechnology Conference and Trade Show, Vol. 2 230 (2005).
[29] M. Freitag, A. T. Johnson, S. V. Kalinin, and D. A. Bonnell, Phys. Rev. Lett. **89**, 216801 (2002).
[30] M. C. Payne, M. P. Teter, D. C. Allan, D. C. Arias, and J. D. Johannopoulos, Rev. Mod. Phys. **64**, 1045 (1992); V. Milman,

B. Winkler, J. A. White, C. J. Pickard, M. C. Payne, E. V. Akhmatskaya, and R. H. Nobes, Int. J. Quantum Chem. **77**, 895 (2000).

[31] J. P. Perdew, J. A. Chevary, S. H. Vosko, K. A. Jackson, M. R. Pederson, D. J. Singh, and C. Fiolhais, Phys. Rev. B **46**, 6671 (1992).

[32] J. A. White and D. M. Bird, Phys. Rev. B **50**, R4954 (1994).

[33] D. Vanderbilt, Phys. Rev. B **41**, R7892 (1990).

[34] H. J. Monkhorst and J. D. Pack, Phys. Rev. B **13**, 5188 (1976).

[35] K. Kunc and R. M. Martin, Phys. Rev. Lett. **48**, 406 (1982).

[36] C. W. Chen, M. H. Lee, and S. J. Clark, Nanotechnology **15**, 1837 (2004).

[37] S. Reich, C. Thomsen, and P. Ordejon, Phys. Rev. B **65**, 155411 (2002).